Journal of Luminescence 44 (1989) 223–231
North-Holland, Amsterdam

OPTICAL PROPERTIES OF QUANTUM WELLS AND SUPERLATTICES UNDER ELECTRIC FIELDS

E.E. MENDEZ and F. AGULLÓ-RUEDA *

IBM Research Division, T.J. Watson Research Center, Yorktown Heights, NY 10598, USA

Received 18 August 1989
Accepted 31 August 1989

We review the effects of a longitudinal electric field on the optical properties of semiconductor quantum wells and superlattices, emphasizing recent developments on the latter, such as the observation of the Stark ladder, field-induced localization, and change in dimensionality of superlattice excitons.

1. Introduction

The application of an external electric field to a semiconductor affects drastically its optical properties, by broadening interband transitions and producing oscillatory structure in their neighborhood (Franz–Keldysh effect), and by weakening, and even destroying, the binding of electrons to impurity or excitonic states. This field-induced ionization of excitons and the subsequent spatial separation of both types of carriers limited for many years optical studies of semiconductors under high fields, especially radiative-recombination processes.

The realization that the confinement of electrons and holes provided by the potential barriers of a quantum well can overcome those limitations [1] has made possible to application of longitudinal fields (perpendicular to well interfaces) larger than 10^5 V/cm, offering new vistas in semiconductor physics and providing opportunities for novel electro-optical devices. More recently, the observation of Stark ladders in superlattices under electric fields and the field-induced localization of electronic carriers [2] has brought new momentum to the field of semiconductor electro-optics, opening the door, once more, to new applications.

This article highlights the major effects of a static longitudinal electric field on the optical properties of quantum wells and superlattices, emphasizing the latest developments. Since several papers have already reviewed the effects of a field in isolated quantum wells [3–5], we limit ourselves to a summary of the main results in section 2. The formation of Stark ladders and field-induced localization in superlattices, as demonstrated by optical experiments, is considered in sect. 3. Finally, sect. 4 discusses important consequences of these effects, namely, variable quantum coherence of the electronic wavefunctions, "blue" shift of the emission and absorption spectra, and a change in the dimensionality of excitons.

2. A quantum well in an electric field: the Stark effect

An electric field, $\mathscr{E}$, perpendicular to the material interfaces of a quantum well couples states of opposite parity, producing second-order effects in their energies and wavefunctions. Thus, the ground-state energy is decreased and the electron (hole) wavefunction is polarized opposite to (along) the direction of the field, as indicated in

* Permanent address: Institute of Materials Science of Madrid (CSIC) Spain.

fig. 1. As in atomic physics, we refer to this double effect on an isolated quantum well as *Stark effect*, because of its analogy with that of an electric field on an isolated atom. Perturbation-theory calculations that assume infinite barrier height yield for the shift of the ground state [6],

$$\Delta E_1^{(2)} = -2.19 \times 10^{-3} \frac{m^* e^2 \mathscr{E}^2 L^4}{\hbar^2} \qquad (1)$$

where m^* is the effective mass and L is the well width. This approximate result, although valid only for weak fields ($e\mathscr{E}L \ll \hbar^2\pi^2/2m^*L^2$), illustrates the direct dependence of the Stark shift on the effective mass and, most of all, on the well width.

Calculations applicable to a broader range of fields, whether variational [6] or quasi-exact treatments based on transmission-probability [7] or transfer-matrix [8] formalisms, confirm that qualitative dependence and show that the finiteness of the potential barrier drastically enhances the effect of the field. As an example, a field of 10^5 V/cm shifts the electron (hole) states of a 100 Å GaAs–$Ga_{0.65}Al_{0.35}As$ quantum well by -6 meV (-15 meV); the shift becomes as large as -55 meV (-81 meV) for a 250 Å well.

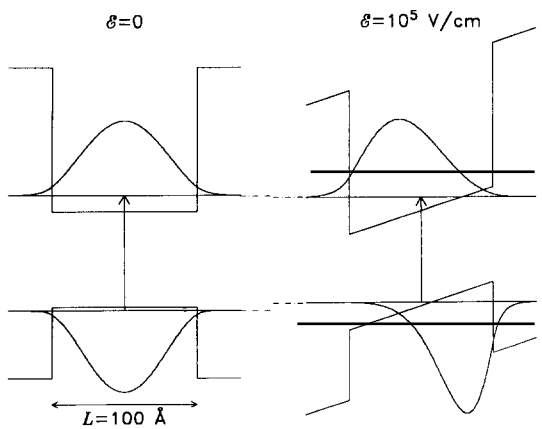

Fig. 1. Schematic representation of the conduction- and valence-band quantum wells of a typical semiconductor double heterostructure such as GaAlAs–GaAs–GaAlAs, showing the wavefunctions and energies of the ground states in the absence of (left) or in the presence of (right) an electric field perpendicular to the heterostructure interfaces. The figure is scaled to show the effects of a field of 10^5 V/cm on a 100 Å GaAs–$Ga_{0.65}Al_{0.35}As$ quantum well.

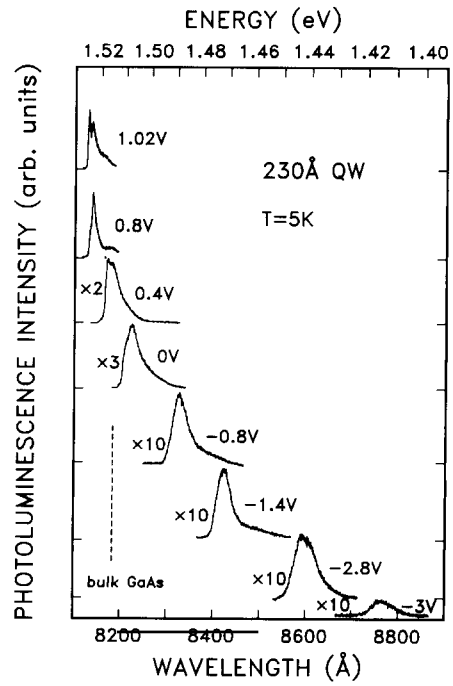

Fig. 2. Photoluminescence spectra of a 230 Å GaAs–$Ga_{0.65}Al_{0.35}As$ quantum well for various electric fields applied via a Schottky-barrier configuration. The field induces large shifts of the luminescence peaks to lower energies and decreases their intensities as a result of the Stark effect (adapted from ref. [8]).

The Stark effect was first proposed to explain the field-induced shift and quenching of the photoluminescence of narrow GaAs–GaAlAs quantum wells [1]. Since then, a variety of optical experiments (absorption [9], photoconductivity [10], Raman scattering [11], photoluminescence excitation [12], etc.) have confirmed the Stark shift and polarization effect and shown their significance in wide wells, in which shifts in the fundamental interband transition of over 100 meV have been observed, as exemplified in fig. 2 by the photoluminescence spectra of a 230 Å GaAs quantum well imbedded in a Schottky diode. The strong dependence of the Stark shift with well width is shown in fig. 3, where experimental results for three different thicknesses are compared with variational and transfer-matrix calculations [8].

The electric field shifts not only the ground level of the quantum well but also its excited

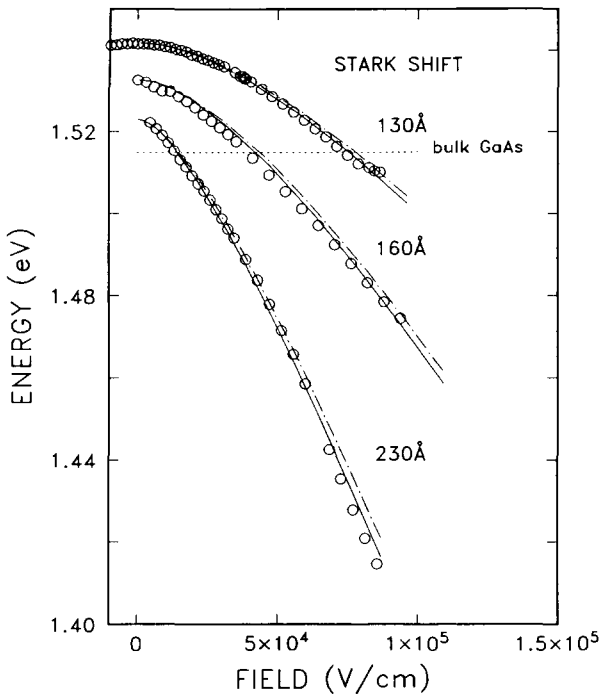

Fig. 3. Comparison between experimental Stark shifts (circles) of GaAs–$Ga_{0.65}Al_{0.35}As$ quantum wells of various widths with calculated shifts. Continuous lines correspond to transfer-matrix calculations whereas discontinuous lines are for variational results (from ref. [8]).

states, although the sign of the shift of the first excited state is generally opposite and the magnitude smaller. Infrared absorption [13] experiments in 120 Å wells under $\mathscr{E} \leqslant 3.5 \times 10^4$ V/cm, have shown positive shifts of up to 1.5 meV for the inter-subband transition involving the ground and first excited states, as a result of the opposite Stark shift of both levels.

The polarization, without complete separation, of electrons and holes induced by the field has two important consequences: an increase of the radiative recombination lifetime and a decrease of the exciton binding energy. The former effect is significant, as demonstrated by time-resolved luminescence experiments [14] in wells wider than 100 Å. (A competing effect, the tunneling of carriers out of the quantum well, dominates the time constants for thin wells, causing an apparent reduction of the decay time [15]). The effect of the field on the exciton binding energy is also appreciable for wells over 100 Å, reducing its value by almost 50% for $L = 200$ Å at $\mathscr{E} = 10^5$ V/cm (ref. [16]).

The capability of excitons in quantum wells to sustain high electric fields, together with their large binding energy, has made possible novel applications that take advantage of the Stark shift in the absorption coefficient, to produce room-temperature modulators [9] with switching times down to 131 ps (ref. [17]) and self-electro-optic devices formed, for example, by a modulator connected in series with a resistor to produce optical bistability [18]. Similarly, frequency and amplitude-tunable lasers have been proposed [1,19] and some of them have already been demonstrated experimentally [20]. Ultrafast optically nonlinear structures have also been suggested, employing wells subject to an electric field and excited by photons of energy below the fundamental energy gap, which screen the field by virtual electron–hole polarization [21,22].

The fundamental effects of an electric field just summarized, although originally demonstrated in GaAs–GaAlAs wells, have been observed in other III–V material systems that may be advantageous for certain optical applications, such as InGaAs–InAlAs [23], InGaAs–InP [24], InGaAsP–InP [25] and GaSb–GaAlSb [26], and in wide-gap II–VI compounds like ZnSe–ZnMnSe [27].

3. A superlattice in an electric field: the Stark ladder

The effects of an electric field on the optical properties of superlattices are best understood by considering first the simple case of a double quantum well. The degeneracy of the states of a system formed by two identical wells is broken if there is coupling between them. Thus, the ground state of an individual well is split into "bonding" and "antibonding" states, whose corresponding wavefunctions are spread throughout the double-wall structure. In practice, such a coupling exists when the barrier between the wells is narrow (typically less than 50 Å), so that the electronic wavefunction of either well has a significant amplitude in the barrier.

An electric field perpendicular to the well planes reduces and eventually destroys that coupling, producing an increase of the energy-level separation, linear with $\mathscr{E}$. Simultaneously, the wavefunctions are gradually localized [28], until at very high fields, once localization into individual wells is complete, the quadratic Stark effect may become significant. These effects have been demonstrated experimentally by absorption [29] and luminescence excitation [30] spectroscopy, which has revealed interband transitions between "bonding" and "antibonding" states of the valence and conduction bands and their dependences with $\mathscr{E}$.

In a material system formed by a periodic array of N identical, interacting wells, with periodicity D, the energy spectrum is formed by N discrete energy levels whose separation decreases with the number of wells. In the limit of very large N (*superlattice*) the spectrum is quasi-continuum, forming a miniband centered around the eigenenergy E_0 of an isolated well and with an energy bandwidth Δ, while the electronic wavefunctions are extended throughout the entire superlattice (see fig. 4(a)).

An electric field $\mathscr{E}$ along the axis of the superlattice decreases coupling between quantum wells, which is at the origin of miniband formation, and produces a splitting of each miniband into discrete states with energies given by $E_0 \pm ne\mathscr{E}D$ ($n = 0, \pm 1, \pm 2, \ldots$), which constitute the so-called Stark ladder. The reduced coupling produces a partial localization of the extended superlattice states to a region $\Delta/e\mathscr{E}$ and an oscillatory motion of frequency $e\mathscr{E}D/h$ (Bloch oscillation). These ideas, explicitly stated long ago for crystalline solids in general [31], so far had evaded observation. Indeed, some of the concepts stirred controversy for some time, and, for example, the very existence of the Stark ladder had been disputed [32]. Several groups have suggested that those effects, were they to exist, should be more easily observable in semiconductor superlattices [33–35].

In a three-dimensional solid, in which D is of the order of Å and Δ of eV, respectively, the electron is confined, for any realistic field ($\mathscr{E} < 10^6$ V/cm), to a region that would include many atomic sites. In contrast, in a superlattice, with a period of ~60 Å and Δ around 0.06 eV, the electronic motion can be restricted to distances of the order of D for moderately high electric fields, $\mathscr{E} \sim 10^5$ V/cm.

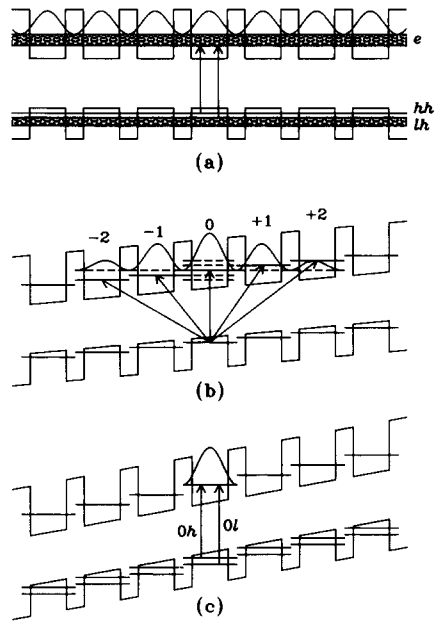

Fig. 4. Conduction- and valence-band profiles for a GaAs–$Ga_{1-x}Al_xAs$ superlattice in the absence (a), or in the presence of an electric field (b), (c), along the superlattice direction. At $\mathscr{E} = 0$, the electron and hole wavefunctions are delocalized and interband transitions take place between minibands. At moderate fields (b), electron and light-hole states are partially delocalized whereas heavy holes are fully localized. Interband transitions involve Stark-ladder states like the ones represented here for the conduction band. For simplicity we have not included in the figure the Stark-ladder states associated with light holes. At high fields (c), all states are completely localized and transitions take place between levels corresponding to isolated quantum wells. The diagrams are scaled for a 40 Å–20 Å superlattice with $x = 0.35$, and fields of 2×10^4 V/cm (b), and 10^5 V/cm (c).

Optical experiments are most suitable to study the formation of Stark ladders, since each level gives rise to an interband transition with a characteristic energy, which in turn varies linearly with electric field. The energies of interband transitions between conduction- and valence-band Stark states of indices n and m, respectively, are given by [2]

$$E_{nm}(\mathscr{E}) = E_{00}(\mathscr{E}) + (n-m)e\mathscr{E}D \quad (n, m = 0, \pm 1, \pm 2, \ldots), \tag{2}$$

where E_{00} is the intrawell ($n - m = 0$) transition energy in the isolated-well limit.

Photoluminescence and photocurrent measurements in GaAs–GaAlAs heterostructures have recently provided the first observation of the Stark ladder in semiconductor superlattices [2]. In that system, as in most other III–V heterostructures, the valence-band ground state corresponds to a heavy-hole state, so that the corresponding miniband has a bandwidth Δ_h much smaller than either the electron or light-hole minibands' widths. Consequently, the localization field, $\mathscr{E}_1 = \Delta/eD$, is considerable lower for heavy holes than for electrons, and there is a field range in which heavy holes are fully localized while electrons are partially extended.

This intermediate-field range is illustrated in fig. 4(b) for $\mathscr{E} = 2 \times 10^4$ V/cm applied to a GaAs–GaAlAs superlattice with 40 Å wells and 20 Å barriers. The electron wavefunction associated with well *0* spreads significantly, although with decreasing amplitude, to several adjacent wells. Similarly, states with wavefunctions centered in neighboring wells (e.g., ± 1, ± 2) have appreciable amplitudes at 0. In contrast, the corresponding hole wavefunctions are confined to individual wells. Then, a hole localized in one particular well, let us say 0, can undergo an optical transition not only with an electron entered in the same well (intrawell transition), but also with other states of the electronic Stark ladder, centered in different wells (interwell transition). These transitions, sometimes called "non-vertical", are characterized by shifts relative to the intrawell transition in units of $e\mathscr{E}D$ ($\nu e\mathscr{E}D$, $\nu = 0, \pm 1, \pm 2, \pm 3 \ldots$), and their observation constitutes the clearest demonstration of the Stark ladder.

Figure 5 shows low-temperature photocurrent (PC) spectra of a 60 Å superlattice for various electric fields. In the intermediate-field regime up to seven structures equally separated in energy can be identified simultaneously, corresponding to an intrawell and six interwell transitions. Their labels in the figure represent the Stark-ladder indices relative to the intrawell transition. With increasing field, the higher-index structures decrease in intensity and eventually disappear, as a reflection of the increasing confinement of the electron wavefunctions.

The energy positions of the PC structures of

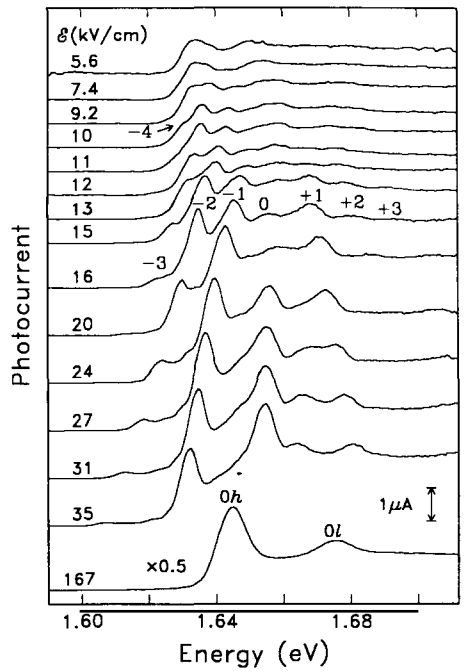

Fig. 5. Low-temperature ($T = 5$ K) photocurrent spectra (offset vertically for clarity) of a 60-Å-period GaAs–$Ga_{0.65}Al_{0.35}As$ superlattice at various electric fields. The labels at intermediate fields represent the indexes of the Stark ladder for electrons, and at very high fields indicate the transitions between fully localized hole and electron states (from ref. [43]).

fig. 5 are summarized in fig.6 as a function of field, for transitions involving both heavy and light holes. In the former set up to nine branches are observed at low fields, emerging from the spectral region covered by the miniband (between full squares) at zero field and with slopes proportional to their Stark index. Although not as complete, a "fan chart" of similar characteristics is obtained for light-hole transitions. It should be noted that in this case some difference exists from the heavy-hole transitions, since both the electrons and light holes are partially delocalized at moderate fields.

As observed in fig. 5, at very high fields the PC spectra consist of two structures, labelled *0*h and *0*l, on a step-like background. These two features, corresponding to intrawell transitions for heavy and light holes, respectively, are the only ones that remain at fields well above the localization field of electrons and holes (~ 120 kV/cm for the hetero-

structure of fig. 5), that is, when both types of carriers are fully confined to individual wells, as sketched in fig. 4(c). At such high fields, even for wells as narrow as those that form a superlattice, the quadratic Stark effect of an isolated well becomes appreciable and leads to small "red" shifts of the *0*h and *1*l transitions, appreciable in fig. 5.

Although the intensities of the high-index structures in fig. 5 decrease monotonically with increasing $\mathscr{E}$ at high fields, the behavior is much more complicated at low fields. For example, at $\mathscr{E} = 13$ kV/cm the -2 transition dominates the spectrum, whereas at 20 kV/cm -1 is dominant. Tight-bonding calculations of the superlattice wavefunctions under a field have predicted the general behavior of the absorption spectra, with their multiple steps for the various transitions [36]. However, since those calculations did not include the coulombic interaction between electron and holes, a direct comparison with experimental spectra, in which excitonic features are dominant, is not possible. A more recent calculation that includes that interaction, although subject to some approximations, represents a first attempt to estimate the relative strength of the exciton structures [37].

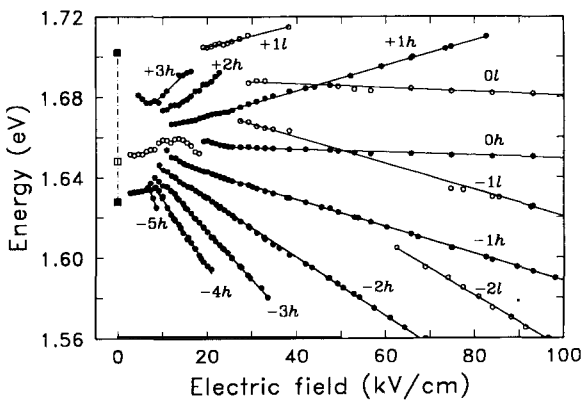

Fig. 6. Experimental interband transition energies as a function of electric field for the superlattice whose photocurrent spectra are shown in fig. 5. Full (empty) circles correspond to transitions between heavy-hole (light-hole) and conduction band states. Full (empty) squares indicate the edges of interband transitions at $\mathscr{E} = 0$ that involve electron and heavy- (light-) hole minibands. Straight lines are least-squares fits to the experimental points (adapted from ref. [43]).

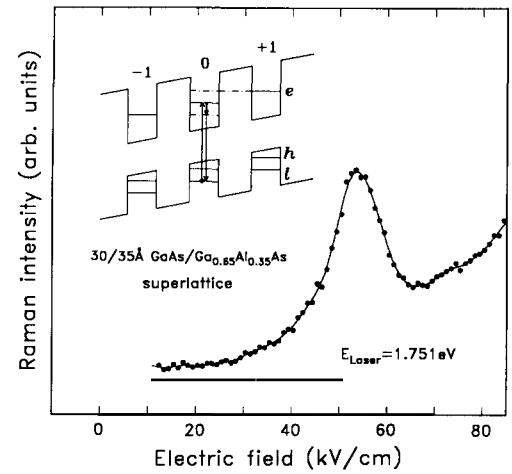

Fig. 7. Raman intensity of the LO GaAs phonon as a function of electric field for a 30 Å–35 Å GaAs–$Ga_{0.65}Al_{0.35}As$ superlattice, for an incident photon energy of 1.751 eV. The strong enhancement of the Raman intensity at ~ 55 kV/cm is due to a double-resonance condition induced by the $n_1 = 0$ and $n_2 = -1$ states of the Stark ladder, sketched in the inset in simplified form.

The Stark-ladder states of a superlattice can also be probed by Raman scattering. The cross section for Raman scattering is enhanced by several orders of magnitude when the energies of the incident and scattered photon both coincide with two electronic transitions, thus achieving double resonance. This condition requires the existence of three states, two of them separated by the energy of a phonon. Two Stark-ladder states, combined with a valence-band state, can provide such a resonance whenever the separation of Stark states of indices n_1 and n_2 equals a phonon energy E_{phon} (see inset of fig. 7), that is, when

$$\mathscr{E}(kV/cm) = 100E_{\text{phon}}(\text{MeV})/D(\text{Å})(n_1 - n_2), \tag{3}$$

Light-scattering measurements in 60 Å-period GaAs–GaAlAs superlattices have demonstrated this field-induced double resonance [38]. A summary of the results is shown in fig. 7, where the intensity of the peak corresponding to a GaAs longitudinal optical phonon is plotted as a function of the electric field for an incident photon energy of 1.751 eV. This energy corresponds to the separation between the $n_1 = 0$ Stark state of the

conduction band and the heavy-hole valence state (which is fully localized at small fields), so that Raman scattering is at least singly resonant at all fields. When $\mathscr{E}$ satisfies eq. [3] for $n_1 = 0$ and $n_2 = -1$, that is, when $\mathscr{E} = 55$ kV/cm, the double-resonance condition produces a drastic enhancement of the Raman intensity, as seen in fig. 7. A similar resonance for $n_2 = -2$ at $\mathscr{E} = 27.5$ kV/cm, although in principle possible, has not been observed.

Photoluminescence [2], photoluminescence excitation [2] and electroreflectance [39] measurements have also revealed the Stark ladders in GaAs–GaAlAs superlattices. However, the complex nature of those processes masks in part the beauty and simplicity of absorption (or absorption-like) spectra. A smaller number of the members of the Stark ladder has been observed by absorption experiments in GaInAs–GaAlInAs [10]. Non-optical techniques, such as deep-level transient spectroscopy [41] and tunneling [42], have also provided limited evidence of Stark states in superlattices.

4. Consequences of the Stark localization

The Stark-ladder states give rise to features in the absorption or photocurrent spectra that shift linearly with $\mathscr{E}$, and eventually disappear at high field. But, in addition, a comparison between high-field and zero-field spectra (see fig. 5) reveals a shift to higher energies of the absorption edge. Such a "blue" shift is a direct consequence of the breakage of the superlattice minibands into localized states in the high-field limit [33]. At $\mathscr{E} = 0$, the energies of the interband transitions T_1 and T_2 (see fig. 4(a)) for heavy and light holes, respectively, correspond to the differences between the bottom of the conduction miniband and the top of the valence minibands. On the other hand, when $\mathscr{E} > \mathscr{E}_1$ the corresponding transitions involve states localized in uncoupled wells (fig. 4(c)). Since the energies of these levels are to first approximation at the center of the superlattice minibands, the transition energies at high fields will increase by $(\Delta_e + \Delta_{hh})/2$ and $(\Delta_e + \Delta_{lh})/2$, respectively.

The "blue" shifts in fig. 5 amount to 15 meV and 26 meV, values that, although quite significant, are less than those to be expected, once we consider that in that case $\Delta_e = 70$ mev, $\Delta_{hh} = 4$ meV and $\Delta_{lh} = 58$ meV when the following parameters are used in a simple Kronig–Penney calculation: 0.31 eV (0.19 eV) for the conduction (valence) band barrier heights, and 0.067 (0.089), 0.34 (0.51), and 0.094 (0.12) for the effective masses of electrons, heavy holes, and light holes in the well (barrier), in units of the free-electron mass. The origin of the differences is at least two-fold. On the one hand there is the quadratic Stark shift, that becomes increasingly important at high fields, reaching 13.8 meV (17.4 meV) for the heavy (light) hole transitions at 250 kV/cm. On the other hand, there is a localization-induced increase of the exciton binding energy.

In the absence of an electric field, since the electrons and holes are itinerant throughout the superlattice, the binding energy of the excitons is not very different to that of bulk semiconductors; for $D = 60$ Å it is about 6 meV. The field-induced localization reduces the spatial extent of the electrons and holes, producing an increase in the excitonic energy, and, under complete localization, the exciton becomes quasi-two-dimensional [43]. Such a change in dimensionality is illustrated in fig. 8 for a 40 Å–40 Å superlattice, where the binding energy, measured from the difference between the exciton peak and the continuum of PC spectra, is plotted against the electric field. Variational calculations of the intrawell excitonic energies [36], within the envelope-function approximation, have been able to reproduce the observed three-to-two-dimensional transition, as shown in fig. 8.

Another important consequence of the formation of Stark ladders is an oscillatory behavior of the optical absorption as a function of the electric field, for fixed photon energy $\hbar\omega$. According to eq. [2], whenever $\mathscr{E}$ is such that

$$\hbar\omega = E_0 + \nu e \mathscr{E}_\nu D (\nu = \pm 1, \pm 2, \ldots), \tag{4}$$

there is an enhancement in the absorption coefficient produced by the transition of index ν. Such an increase, which is periodic in the reciprocal of the field, leads to several regions of strong nega-

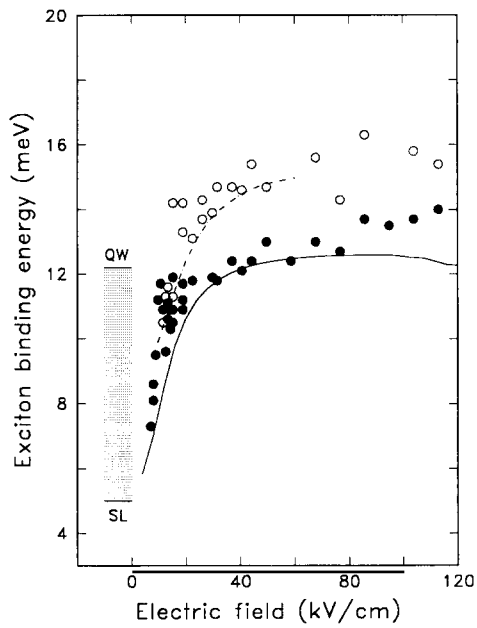

Fig. 8. Exciton binding energy as a function of electric field in a 40 Å–40 Å GaAs–$Ga_{0.65}Al_{0.35}As$ superlattice. Full (empty) circles are for heavy- (light-) hole excitons. The solid (dashed) curve represents the calculated values for the heavy- (light-) hole exciton. The shaded area depicts the expected range for the heavy-hole exciton binding energy: between the superlattice (SL) and the isolated quantum well (QW) limits at zero field.

tive differential resistance in the photocurrent–voltage characteristics of p-i-n structures, as demonstrated recently [43].

Finally, the observation of Stark-ladder transitions provides a direct measurement of the quantum coherence of the superlattice wavefunctions. In real superlattices, even in the absence of any electric field, there is a certain degree of wavefunction localization created by deviations from perfect periodicity, caused, e.g., by well-width or barrier-height fluctuations. Under strong localization the wavefunction coherence can be reduced to a few periods and even to a single well. As has been described above, in the presence of an electric field the number of interwell transitions involving heavy holes measures directly the spatial extent of the electronic states at that field, and consequently extrapolation to zero-field gives their maximum coherence.

For the 60 Å-period superlattice of fig. 5, the electron wavefunctions remain coherent at $\mathscr{E}=0$ for at least ten periods, in view of the ten different transitions that can be resolved at very low fields. (Although only nine heavy-hole transitions are represented in fig. 5, a tenth one, corresponding to $\nu=-6$, was resolved as a negative-resistance feature in the photocurrent characteristics [44].) This large coherence is maintained for temperatures of at least up to 200 K, suggesting that it is not restricted by inelastic scattering. The actual limit may be due to the small fluctuations in layer thickness or alloy composition, which seem to affect much more to superlattices with long period, once inhomogeneous broadening becomes comparable to the superlattice bandwidths. Indeed, measurements in heterostructures with $60 \leqslant D \leqslant 85$ Å have demonstrated that coherence is gradually reduced with increasing D, to two or three periods [44].

The observation of coherence even at room temperature makes Stark-ladder effects attractive for applications. Thus, the localization-induced blue shift has been used recently to obtain large absorption modulation in a self-electro-optic device [45].

The developments of the last few years reviewed here have contributed to a better understanding of very basic ideas in the theory of solids under electric fields, and have proved concepts that were once quite controversial, such as the Stark ladder. To a large extent these advances have been possible by a dramatic improvement in material's quality, as attested by the demonstration of long electronic coherence in artificial superlattices. Novel structures based on them that take advantage of their reduced Brillouin zones will undoubtedly follow, not only for optical applications but also for devices based on transport along the superlattice direction.

Acknowledgements

This work has been supported in part by the Army Research Office. One of us (FAR) has benefitted from a fellowship of the Microelectronics Program of the Spanish Ministry of Education and Science.

References

[1] E.E. Mendez, G. Bastard, L.L. Chang, L. Esaki, H. Morkoç and R. Fischer, Phys. Rev. B26 (1982) 7101, and Proc. 16th Int. Conf. Phys. Semicond., Montpellier (1982) Physica B117&118 (1983) 711.

[2] E.E. Mendez, F. Agulló-Rueda, and J.M. Hong, Phys. Rev. Lett. 60 (1988) 2426.

[3] D.A.B. Miller, J.S. Weiner and D.S. Chemla, IEEE J. Quant. Electron QE-22 (1986) 1816.

[4] G. Bastard, in: Interfaces, Quantum Wells and Superlattices, eds. C.R. Leavens and R. Taylor, (Plenum, New York, 1988) p. 227.

[5] D.A.B. Miller, D.S. Chemla, and S. Schmitt-Rink, in: Optical Nonlinearities and Instabilities in Semiconductors, ed. H. Haug, (Academic Press, New York, 1988) p. 325.

[6] G. Bastard, E.E. Mendez, L.L. Chang and L. Esaki, Phys. Rev. B28 (1983) 3241.

[7] D.A.B. Miller, D.S. Chemla, T.C. Damen, A.C. Gossard, W. Wiegmann, T.H. Wood and C.A. Burrus, Phys. Rev. B32 (1985) 1043.

[8] L. Viña, E.E. Mendez, W.I. Wang, L.L. Chang and L. Esaki, J. Phys. C: Sol. St. Phys. 20 (1987) 2803.

[9] T.H. Wood, C.A. Burrus, D.A.B. Miller, D.S. Chemla, T.C. Damen, A.C. Gossard and W. Wiegmann, Appl. Phys. Lett. 44 (1984) 16.

[10] Y. Masumoto, S. Tarucha and H. Okamoto, Phys. Rev. B33 (1986) 5961.

[11] C. Tejedor, J.M. Calleja, L. Brey, L. Viña, E.E. Mendez, W.I. Wang, M. Staines and M. Cardona, Phys. Rev. B36 (1987) 6054.

[12] L. Viña, R.T. Collins, E.E. Mendez and W.I. Wang, Phys. Rev. Lett. 58 (1987) 832.

[13] A. Harwit and J.S. Harris, Jr., Appl. Phys. Lett. 50 (1987) 685.

[14] H.-J. Polland, L. Schultheis, J. Kuhl, E.O. Göbel and C.W. Tu, Phys. Rev. Lett. 23 (1985) 2610.

[15] J.A. Kash, E.E. Mendez and H. Morkoç, Appl. Phys. Lett. 46 (1985) 173.

[16] J.A. Brum and G. Bastard, Phys. Rev. B31 (1985) 3893.

[17] T.H. Wood, C.A. Burrus, D.A.B. Miller, D.S. Chemla, T.C. Damen, A.C. Gossard and W. Wiegmann, IEEE J. Quant. Electron. QE-21 (1985) 117.

[18] D.A.B. Miller, D.S. Chemla, T.C. Damen, A.C. Gossard, W. Wiegmann, T.H. Wood and C.A. Burrus, Appl. Phys. Lett. 45 (1984) 13.

[19] M. Yamanishi and I. Suemune, Jap. J. Appl. Phys. 22 (1983) L22.

[20] T. Takeoka, M. Yamanishi, Y. Kan and I. Suemune, Jap. J. Appl. Phys. 26 (1987) L117.

[21] M. Yamanishi, Phys. Rev. Lett. 59 (1987) 1014.

[22] D.S. Chemla, D.A.B. Miller and S. Schmitt-Rink, Phys. Rev. Lett. 59 (1987) 1018.

[23] K. Wakita, Y. Kawamura, Y. Yoshikuni and H. Asahi, Electron. Lett. 22 (1987) 907.

[24] M.G. Shorthose, A.C. Maciel, J.F. Ryan, M.D. Scott, A. Moseley, J.I. Davies and J.R. Riffat, Appl. Phys. Lett. 51 (1987) 493.

[25] J.E. Zucker, I. Bar-Joseph, B.I. Miller, U. Koren and D.S. Chemla, Appl. Phys. Lett. 54 (1989) 10.

[26] T.H. Wood, E.C. Carr, C.A. Burrus, R.S. Tucker, T.-H. Chiu and W.T. Tsang, Electron. Lett. 23 (1987) 540.

[27] Q. Fu, Z.V. Nurmikko, L.A. Kolodziejski, R.L. Gunshor and J.-W. Wu, Appl. Phys. Lett. 51 (1987) 578.

[28] E.J. Austin and M. Jaros, J. Phys. C: Sol. St. Phys. 19 (1986) 533.

[29] M.N. Islam, R.L. Hillman, D.A.B. Miller, D.S. Chemla, A.C. Gossard and J.H. English, appl. Phys. Lett. 50 (1987) 1098.

[30] H.Q. Le, J.J. Zayhowski and W.D. Goodhue, Appl. Phys. Lett. 50 (1987) 1510.

[31] H.M. James, Phys. Rev. 76 (1949) 1611. For a more explicit formulation of the Stark-ladder concept see, e.g., G.H. Wannier, in: Elements of Solid State Theory (Cambridge, Univ. Press, 1959) p. 190.

[32] J. Zak, Phys. Rev. Lett. 20 (1968) 1477.

[33] L. Esaki and R. Tsu, IBM J. Res. Develop. 14 (1970) 61.

[34] P.W.A. McIlroy, J. Appl. Phys. 59 (1986) 3532.

[35] E. Cota, J.V. José and G. Monsiváis, Phys. Rev. B35 (1987) 8929.

[36] J. Bleuse, G. Bastard and P. Voisin, Phys. Rev. Lett. 60 (1988) 220.

[37] J. Brum and F. Agulló-Rueda, in: Proc. 8th Int. Conf. on Electron. Prop. Two-Dimensional Systems, Grenoble, Sept. 1989; Surf. Sci., to be published.

[38] F. Agulló-Rueda, E.E. Mendez and J.M. Hong, Phys. Rev. B38 (1988) 12720.

[39] P. Voisin, J. Bleuse, C. Bouche, S. Gaillard, C. Alibert and A. Regreny, Phys. Rev. Lett. 61 (1988) 1639.

[40] J. Bleuse, P. Voisin, M. Allovon and M. Quillec, Appl. Phys. Lett. 53 (1988) 2632.

[41] S.L. Feng, J.C. Bourgoin and G.G. Qin, Appl. Phys. Lett. 54 (1989) 532.

[42] P. England, M. Helm, J.R. Hayes, J.P. Harbison, E. Colas and L.T. Florez, Appl. Phys. Lett. 54 (1989) 647.

[43] F. Agulló-Rueda, J. Brum, E.E. Mendez and J.M. Hong, not published.

[44] F. Agulló-Rueda, E.E. Mendez and J.M. Hong, Phys. Rev. B40 (1989) 1357.

[45] I. Bar-Joseph, K.W. Goossen, J.M. Kuo, R.F. Kopf, D.A.B. Miller and D.S. Chemla, Appl. Phys. Lett. 54 (1989) 340.